International Journal of Pharmaceutics 431 (2012) 111–119

Contents lists available at SciVerse ScienceDirect

International Journal of Pharmaceutics

journal homepage: www.elsevier.com/locate/ijpharm

Insight into the solubility and dissolution behavior of piroxicam anhydrate and monohydrate forms

Urve Paaver[a], Andres Lust[a], Sabiruddin Mirza[b], Jukka Rantanen[c], Peep Veski[a], Jyrki Heinämäki[a], Karin Kogermann[a,*]

[a] Department of Pharmacy, Faculty of Medicine, University of Tartu, Nooruse 1, 50411 Tartu, Estonia
[b] Division of Pharmaceutical Technology, P.O. Box 56 (Viikinkaari 5E), 00014 University of Helsinki, Helsinki, Finland
[c] Department of Pharmacy, Faculty of Health and Medical Sciences, University of Copenhagen, Universitetsparken 2, 2100 Copenhagen, Denmark

ARTICLE INFO

Article history:
Received 21 January 2012
Received in revised form 26 March 2012
Accepted 16 April 2012
Available online 23 April 2012

Keywords:
Piroxicam
Dissolution
Hydrate formation
Solubility
Supersaturation
Nucleation

ABSTRACT

The aim of the present study was two-fold: (1) to investigate the effect of pH and presence of surfactant sodium lauryl sulphate (SLS) on the solubility and dissolution rate of two solid-state forms of piroxicam (PRX), anhydrate (PRXAH) and monohydrate (PRXMH), and (2) to quantitatively assess the solid-phase transformation of PRXAH to PRXMH in slurry with a special interest to the impact on the solubility and dissolution behavior of the drug. X-ray powder diffractometry (XRPD), Raman spectroscopy and scanning electron microscopy (SEM) were used for characterization of the solid-state forms. Phase transformation was monitored in slurry by means of in-line Raman spectroscopy, and the partial least squares (PLS) regression model was used for predicting the amount of PRXMH. The results showed that the solubility and dissolution rate of PRXAH were higher compared to PRXMH at different pHs. The pH and presence of SLS together affected the solubility and dissolution rate of different PRX forms. The lowest solubility values and dissolution rates for PRX forms were observed in distilled water (pH 5.6) at 37 °C. The changes in the dissolution rate could be explained by the hydrate formation during solubility testing. The rate of hydrate formation was also dependent on the pH of the dissolution medium.

1. Introduction

Solid phase transformations including solvated and hydrated phases of active pharmaceutical ingredients (APIs) may have a profound impact on the physicochemical, pharmaceutical and biopharmaceutical properties, such as solubility, dissolution rate, chemical stability and bioavailability of API. Since oral bioavailability of many poorly water soluble APIs depend upon solubility and dissolution rate, identification and detection of such transformations between hydrate forms of APIs in bulk state and pharmaceutical formulations, are important. Unstable formulations, called supersaturating drug delivery systems (SDDS), where an API exists in metastable state such as amorphous form, solid dispersion or other less stable solid form (depending on the conditions either anhydrate/hydrate or a metastable polymorph), are likely to have phase transformations *in vivo*. These formulations act by giving a supersaturated solution after fast dissolution of a metastable form and increasing the absorption and consequently the bioavailability of an API. In order to improve the solubility-limited bioavailability of APIs, these SDDS need to be stabilized by preventing their precipitation from supersaturated solution (Brouwers et al., 2009; Zimmermann et al., 2008).

Solubility and dissolution tests are considered as routine *in vitro* performance tests for solid dosage forms. However, it has been reported that during dissolution testing, the solid state conversions of APIs (*e.g.* hydrate formation) may occur resulting in misinterpretation of the results. Such misinterpretations due to the solvent-mediated hydrate formation have been reported with, *e.g.* theophylline, nitrofurantoin and amlodipine (Aaltonen et al., 2006; De Smidt et al., 1986; Koradia et al., 2011; Otsuka et al., 1992). Vibrational spectroscopic techniques could provide a valuable insight into the solid state behavior of the API in the presence of biorelevant dissolution media and surfactants (Lehto et al., 2009). Similarly, during processing a process induced transformations and related precipitation of an API may change the expected outcome (Airaksinen et al., 2005; Zimmermann et al., 2008). Several recent reports provide evidence that unexpected solvent-mediated transformations between the solid hydrates of APIs may be induced especially during the wet processing of pharmaceuticals (Airaksinen et al., 2005; Jørgensen et al., 2002; Otsuka et al., 1997; Zhang et al., 2004; Wikström et al., 2005).

* Corresponding author at: Nooruse 1, 50411 Tartu, University of Tartu, Estonia. Tel.: +372 56 509 455; fax: +372 737 5289.
E-mail addresses: urve.paaver@ut.ee (U. Paaver), andres.lust@ut.ee (A. Lust), sabir.mirza@helsinki.fi (S. Mirza), jtr@farma.ku.dk (J. Rantanen), peep.veski@ut.ee (P. Veski), jyrki.heinamaki@ut.ee (J. Heinämäki), kkogermann@gmail.com (K. Kogermann).

0378-5173/$ – see front matter © 2012 Elsevier B.V. All rights reserved.
http://dx.doi.org/10.1016/j.ijpharm.2012.04.042

Piroxicam (PRX) is a known API that has extensively been used as a model substance due to its interesting properties. Due to the zwitterionic nature of PRX, this molecule can exist in different prototropic forms in a solution (Banerjee and Sarkar, 2002; Chakraborty and Sarkar, 2005) and it has different solid state forms (Sheth et al., 2004; Vrečer et al., 2003). Piroxicam anhydrate (PRXAH) and monohydrate (PRXMH) represent PRX solid state forms with different molecular structures. PRXAH is a neutral form with EZE configuration of the molecules (Kojic-Prodic and Ruzic-Toros, 1982; Vrečer et al., 2003). PRXMH is a zwitterionic form with ZZZ configuration of the molecules (Reck et al., 1988). Thermodynamically anhydrous forms are more active than hydrates. Different inter- and intramolecular bonding and molecular packing change the solubility and dissolution rate of the forms which was also observed in the present study.

PRX can be considered as an amphiphilic drug having $-NH_2$ and $-COOH$ groups and it is known to have two pK_a values (1.86 and 5.46) (Jinno et al., 2000), which contribute to PRX behavior at different pHs. However, most studies consider PRX as a weak acid and its pK_a value is 5.3 (Okuyama et al., 1999). PRX can exist as a cation, as a zwitterion or as an anion depending on the pH of the solution (Banerjee et al., 2003). The degree to which PRX is ionized depends largely on the pH of the medium. At pH 1.2 PRX exists as a cation and acts as an acid. At pH 5.6 and 7.2 PRX is in a neutral/zwitterionic form and can act as an acid or as a base in a solution. It is observed that the zwitterion has the lowest solubility. These observations match also with the dissolution behavior of PRXAH at various pHs. Controversial reports, however, can be found in the literature. According to Yazdanian et al. (2004), PRX can be classified as a Class I drug in Biopharmaceutics Classification System (Amidon et al., 1995) based on its solubility. Gwak et al. (2005) suggested that PRX could be classified as a Class II drug. These controversial reports may be due to the fact that during the solubility and dissolution studies of PRX, some unexpected (and unknown) phenomena may take place affecting the behavior of the drug.

Sodium lauryl sulphate (SLS) is an anionic surfactant with a high surface activity and good solubilizing potential. It is commonly used as an excipient in oral formulation for the purpose of increasing the aqueous solubility of poorly water soluble drugs. However, the action is largely dependent on its anionic charge, critical micellar concentration (CMC), interaction with an API (pK_a), and the environment (pH). High amount of SLS should be avoided due to its charged nature and irritation potentials (Zhang and Li, 2004). The effect of SLS on the solubility and dissolution of APIs has been extensively studied in the literature (Bhattachar et al., 2011; Chakraborty et al., 2009; Shihab et al., 1979) as well as its effects in microgels (Zhang and Li, 2004). Surfactant (SLS) can also affect the solid-state phenomena of APIs (Lehto et al., 2009; Luhtala, 1992; Rodriguez-Hornedo and Murphy, 2004). For example, SLS has been found to increase the surface-mediated nucleation of carbamazepine dihydrate with a little effect on its particle morphology (Rodriguez-Hornedo and Murphy, 2004).

The objective of the present study was two-fold: (1) to investigate the effect of pH and presence of SLS on the solubility and dissolution rate of PRXAH and PRXMH, and (2) to assess the solid-phase transformation of PRXAH to PRXMH in slurry with a special reference to the impact on the solubility, dissolution and solvent-mediated transformation behavior of PRX.

2. Materials and methods

2.1. Materials

2.1.1. Preparation of PRX forms

Model substance PRX was obtained from Letco Medical, Inc., USA and was characterized as a mixture of PRX forms I and II by X-ray powder diffractometry (XRPD). PRX monohydrate (PRXMH) was prepared by recrystallization from hot saturated water solution, as described in the literature (Kogermann et al., 2007). Pure anhydrous PRX form I (PRXAH) was prepared by dehydration of PRXMH at 157 °C. All samples were passed through a 150-μm sieve prior to experiments. Distilled water was used in all experiments. Other reagents and solvents obtained from Sigma–Aldrich Inc. were of reagent grade, and were used without further purification.

2.1.2. Preparation of samples for partial least squares (PLS) regression calibration

PLS calibration samples were prepared by gently mixing the two forms of PRX (PRXAH and PRXMH) in different weight ratios, as previously published (Kogermann et al., 2008). The model consisted of 19 mixtures in triplicate with concentrations of 0–100%.

2.1.3. Preparation of the dissolution media

Buffer solutions with different biorelevant pHs were prepared according to USP XXVIII. Solutions with pH 1.2, 5.6 and 7.2 were prepared using HCl/KCl buffer, distilled water and phosphate buffer solutions, respectively. The pH of buffer solutions was confirmed by pH-meter (Hanna Instruments, H19024, Microcomputer pH meter).

2.2. Methods

2.2.1. X-ray powder diffractometry (XRPD)

Crystal structures of all materials (hydrate/anhydrous forms) were verified by XRPD using the diffractometer with Ni filtered Cu Kα radiation (Bruker D8 Advance, Bruker AXS GmbH, Karlsruhe, Germany) and comparing the experimental results to the theoretical patterns in the Cambridge Structural Database (CSD, Cambridge, UK). Scanning steps of 0.01° 2θ from 3° to 50° 2θ and a total counting time of 8.8 s per step were used. The operating current and voltage were 40 mA and 40 kV, respectively. Refcodes BIYSEH (Reck et al., 1988) and CIDYAP01 (Bordner et al., 1984) were used as a reference crystal structures, for PRXAH and PRXMH, respectively.

2.2.2. Karl Fischer (KF) titration

A Karl Fischer titrator (Mettler DL 35, Switzerland) was used to verify the water content (expressed as w/w%) of all the solid-state forms. The standard sample for calibration was an analytical grade sodium tartrate hydrate (water content 15.66%).

2.2.3. Raman spectroscopy

Raman spectra were collected using a Raman spectrometer equipped with a thermoelectrically cooled CCD detector (1024 × 64) and a fiber optic probe (B&W TEK Inc., Newark, USA). The laser source was an enhanced diode laser system (B&W TEK Inc., Newark, USA), which operated at 785 nm. The detection range was between 200 cm^{-1} and 2200 cm^{-1} with a 10-s integration time and each spectrum was the average of 3 scans. BWTek software (BWTek, Inc., Newark, USA) was used for the collection of Raman spectra.

In situ Raman spectroscopy was performed using the same Raman spectrometer. The measurements were carried out using a 300-mW laser source. The integration time was 1 s. Each spectrum was the average of 3 scans. During the slurry experiments the spectra were collected with an interval of 5 min during the time period up to 8 h.

2.2.4. Uv–vis spectroscopy

Absorption spectra of PRXAH and PRXMH in pure distilled water and in the presence of SLS (0.1, 0.5 and 1%) were recorded with ISS-UV/VIS Chem USB4 (Ocean Optics Inc., USA). All samples were measured using a transmission cell setup at a constant temperature

of 22 °C. Baseline correction was performed with distilled water or SLS solutions (0.1, 0.5, 1%) before the measurements.

2.2.5. Scanning electron microscopy (SEM)

The morphology and size of PRX samples were studied by Helios™ NanoLab 600 (FEI Company, USA) high-resolution scanning electron microscope (HR-SEM). A measurement function of the microscope driving program xT Microscope Control (FEI) was used for the dimension measurements. Samples were mounted on aluminum stubs with silver paint and magnetron sputter coated with a 3-nm gold layer in argon atmosphere prior to the microscopy.

2.2.6. Dissolution experiments

Dissolution tests were carried out in a semi-automated dissolution system (Termostat-Sotax AT7, Sotax, Switzerland) according to USP XXVIII basket method (United States Pharmacopoeia, 2005, 2412 S). Hard gelatin capsules (size 1) were manually filled with 20 mg of PRX (either PRXAH or PRXMH). All capsules were weighed before and after capsule filling. The dissolution rate of PRXAH and PRXMH was investigated for 10 h in 900 ml of dissolution medium at 50 rpm and 37 ± 0.5 °C. The samples were filtered through glass microfibre filters (Whatman® GF/D). An aliquot of the release medium (5 ml) was withdrawn at predetermined time intervals (every 3 min). The concentration of the dissolution medium was measured using a UV-Vis spectrophotometer (Ultrospec III, Biochrom Ltd., UK) at a wavelength of 354 nm. Reproducibility was confirmed (six capsules were investigated during one dissolution test and two parallels were performed at each dissolution condition) and error expressed as standard deviation (S.D.). Standard solution was prepared using PRXAH in 0.02 M NaOH solution.

2.2.7. Solubility experiments

The maximum solubility of PRX forms was determined using USP XXVIII method (paddle, 100 rpm) using the same semi-automated dissolution system as for dissolution experiments. PRX powder was added in an excess (200 mg) to 900 ml of dissolution media (pH 1.2, 5.6 and 7.2) and kept at 37 ± 0.5 °C and constant stirring. PRX concentrations in dissolution media were determined every 15 min using UV-Vis spectrophotometer at a wavelength of 354 nm.

2.2.8. In situ slurry experiments

A 2-g sample of pure PRXAH (obtained by heating PRXMH in vacuum-oven for 24 h at temperature of 100 °C and pressure of 7200 Pa) was suspended in 5 ml of buffer solutions (pH 1.2 or 7.2) and distilled water (pH 5.6). Continuous mixing was performed and in-line Raman spectra were collected.

2.3. Data analysis

Data were analyzed using Simca-P (Version 12.0, Umetrics AB, Umea®, Sweden). Qualitative and quantitative analyses were performed using principal component (PCA) and partial least squares (PLS) regression analyses, respectively. PCA enabled to qualitatively evaluate the phase transformation in slurry. PLS regression was used to extract the quantitative information from the spectroscopic data measured during the in-line slurry experiments. A more detailed description of the model development and parameters can be found in a paper by Kogermann et al. (2008). The spectra of pure samples (PRXAH and PRXMH) and the respective binary mixtures, as well as the spectra of PRXAH (before the measurement) and PRXMH (after the measurement) in slurry, were inserted in the PLS model. Two thirds of the data was randomly selected and used to create the model and the remaining third to validate the model. The spectral region of 1105–1632 cm^{-1} was chosen for the analysis. Before PLS regression the PRX spectra were SNV corrected and mean centered. PLS model was constructed using 118 observations and 266 variables, and two latent variables were used for analysis, where the best model fit was obtained. The solubility and dissolution data were compared using a Student's *t*-test of the two samples assuming unequal variances to evaluate the differences.

3. Results and discussion

3.1. Characterization of the forms

XRPD and Raman spectroscopy confirmed the crystal forms of PRX (Fig. 1) and were in good agreement with the theoretical patterns and previously published data (Kogermann et al., 2007). According to KF analysis, the water content of PRXAH and PRXMH was 0.01% and 5.6%, respectively. These results differ only slightly from the theoretical values.

Scanning electron micrographs (SEM) revealed the crystal size, shape and surface properties of the two PRX forms (Fig. 2). Both crystal forms showed similar crystal size, but PRXMH crystals showed much smoother surface of the crystals. As expected (Bordner et al., 1984; Reck and Laban, 1990), both solid-state forms showed similar prismatic crystal shapes. The yellow color of

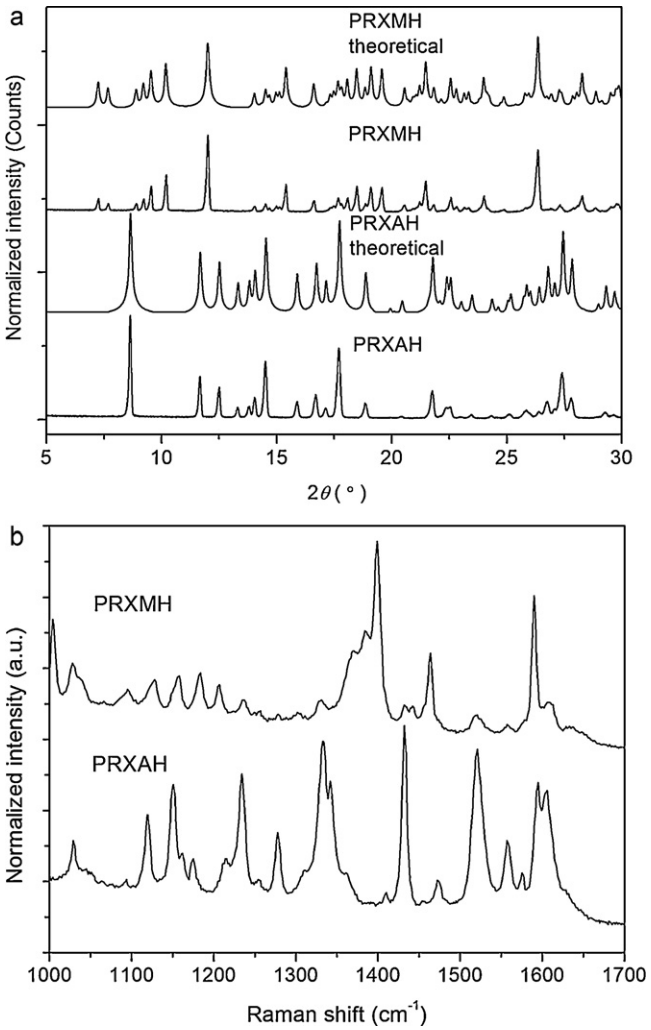

Fig. 1. (a) X-ray diffractometry patterns and (b) Raman spectra of PRXMH and PRXAH. All spectra are normalized and offset for clarity.

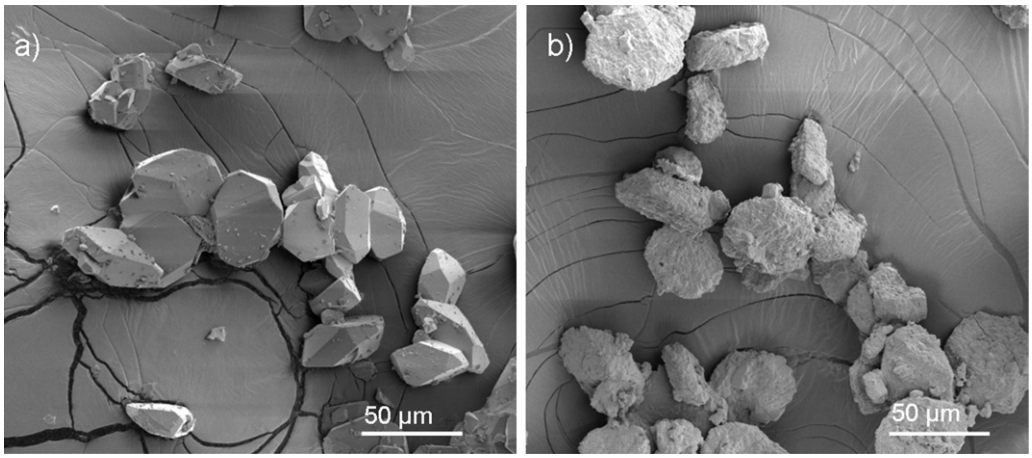

Fig. 2. Scanning electron micrographs of: (a) PRXMH and (b) PRXAH. Magnification of 500×.

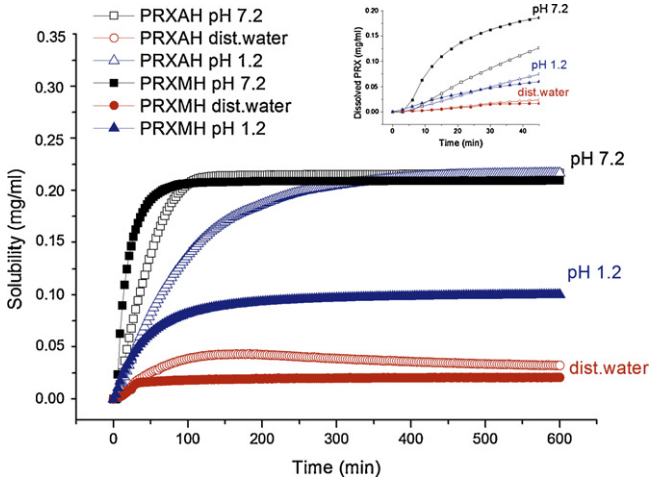

Fig. 3. The solubility-time profiles of PRXAH (open symbols) and PRXMH (closed symbols) at pH 7.2 (black squares), distilled water pH 5.6 (red circles), and pH 1.2 (blue triangles) using 200 mg PRX dose. To clarify presentation, error bars are not shown. S.D. mean absolute values were in the range of 1.5–3.5 for PRXAH and in the range of 1.3–1.8 for PRXMH. (For interpretation of the references to color in this figure legend, the reader is referred to the web version of the article.)

PRXMH due to the zwitterionic structure (Sheth et al., 2005), simplified the visual differentiation of the two PRX solid-state forms.

3.2. Solubility and dissolution of PRX forms

3.2.1. Effect of aqueous medium and pH on the solubility of PRX forms

Solubility is determined by the degree of ionization, molecular size, interactions of substituted groups with solvent and crystal properties. When pH of an aqueous solution approaches the pK_a, there is a very pronounced change in the ionization of an API, and consequently in API's solubility and dissolution. According to the solubility plots (Fig. 3), both PRX forms have the lowest solubility in distilled water (pH 5.6). The highest solubility was observed in phosphate buffer solution (pH 7.2), and both forms showed mid-solubility values at pH 1.2 (HCl/KCl buffer solution). These results are in accordance with the published findings of Jinno et al. (2000) suggesting that the best solubility of PRX would be in basic environment.

As seen in Table 1 and Fig. 3, PRXAH had better solubility and the total amount of API dissolved was higher at all investigated biorelevant pH values than that observed with PRXMH ($p < 0.05$). Only during the initial stages of solubility testing at pH 7.2 (phosphate buffer solution) and 1.2 (HCl/KCl buffer solution), PRXMH showed higher dissolution rates compared to PRXAH (Fig. 3, figure enlargement). Yazdanian et al. (2004) showed that PRX solubility changes with the pH of the testing environment, and the values match with the present study. However, the question remains about the settings of solubility testing. If the testing involves a solvent-mediated phase transformation from PRXAH to PRXMH, then (at the end of the test) the solubility of PRXMH is measured instead of the maximum solubility of PRXAH. Otsuka et al. (1992) reported that during the dissolution of nitrofurantoin anhydrate a phase change to nitrofurantoin monohydrate occurs. Similar behavior has been also reported with phenobarbital (Nogami et al., 1969). Otsuka et al. (1992) proposed that the solubility of anhydrous forms should be carried out using the rotating-disk method in order to avoid the misinterpretations.

It is well known that the zwitterionic form of chemical substance has usually lower solubility. In the present study, PRXMH (zwitterion) exhibited lower solubility compared to PRXAH, and this is in accordance with the previously published results (Vrečer et al., 2003). Kozjek et al. (1985) showed that PRXAH has also better absorption characteristics compared to PRXMH. The molecular structures of PRX in the CSD allow comparison of the two solid-state forms and it is evident that much of the hydrogen bonding functionality in PRXMH (zwitterion) is turned inward to make a hydrogen bonded dimer. This allows explaining the slow dissolution of PRXMH compared to PRXAH. However, in addition to the molecular structure the ionization of the molecules most probably affected the solubility and dissolution rates since at different pHs the dissolution rates of PRX forms changed. As seen

Table 1
Maximum solubility of PRX forms (mg/ml) at different pHs at 37 °C.

PRX form	pH 7.2 (phosphate buffer solution)	pH 5.6 (distilled water)	pH 1.2 (HCl/KCl buffer solution)
PRXAH	[a]	0.043 ± 0.012	[a]
PRXMH	0.210 ± 0.002	0.020 ± 0.002	0.100 ± 0.004

Each data point represents the mean ± S.D. of 2 measurements.
[a] Not possible to measure at these experimental conditions (200 mg dose dissolved in 900 ml dissolution medium).

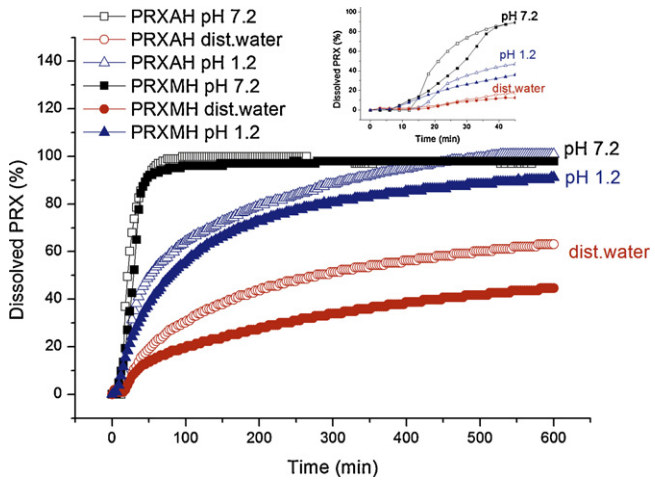

Fig. 4. The dissolution profiles of PRXAH (open symbols) and PRXMH (closed symbols) at pH 7.2 (black squares), distilled water pH 5.6 (red circles) and pH 1.2 (blue triangles) using 20 mg PRX dose. To clarify presentation, error bars are not shown. S.D. mean values were 1.9% (at pH 7.2), 0.8% (distilled water pH 5.6) and 1.3% (at pH 1.2) for PRXAH and 1.9% (at pH 7.2), 0.5% (distilled water pH 5.6) and 1.2% (at pH 1.2) for PRXMH, respectively. (For interpretation of the references to color in this figure legend, the reader is referred to the web version of the article.)

in Fig. 3, both forms showed similar solubility-time profiles. The plateau was reached and therefore maximum values could be calculated. Thus, at pH 7.2 (phosphate buffer solution) and pH 1.2 (HCl/KCl buffer solution) no maximum solubility for PRXAH could be calculated due to the dissolution of all the material (200 mg) in 900 ml of buffer solution within few hours of testing. The time for achieving the maximum solubility varied between the two forms. PRXMH reached the maximum solubility values earlier compared to PRXAH. For example, at pH 5.6 the plateau was obtained and therefore the maximum solubility of PRXMH was reached within 100 min, whereas the complete dissolution for PRXAH was observed after 150 min of testing. To explain these observations, further investigation was performed using dissolution testing of the solid-state forms at various pHs.

3.2.2. *Effect of aqueous medium and pH on the dissolution of PRX forms*

To investigate the effect of biorelevant pH on the dissolution of PRX forms, and consequently, to predict the dissolution behavior in different parts of gastrointestinal tract, the *in vitro* dissolution tests were performed in aqueous media with different pHs. Similarly to the solubility, the dissolution of PRX forms was strongly affected by the aqueous medium and pH. As seen in Fig. 4, significantly faster dissolution was observed with both PRX forms at pH 7.2 (phosphate buffer solution) than at pH 1.2 (HCl/KCl buffer solution) or 5.6 (distilled water). In addition, the plateau was reached only at pH 7.2 (phosphate buffer solution). At pH 1.2 (HCl/KCl buffer solution) and pH 5.6 (distilled water), clear upward trend was observed providing evidence that dissolution was still occurring. Within 8 h, PRX was not completely dissolved at pH 1.2 (HCl/KCl buffer solution) and pH 5.6 (distilled water). This was also supported by the detectable amount of white (PRXAH) or yellow (PRXMH) powder at the bottom of the dissolution vessel.

Dissolution profiles (Fig. 4) provide evidence that there are clear differences in the dissolution rate and total amount of solute dissolved between the two PRX forms. However, according to *t*-test, the differences were not statistically relevant at pH 7.2 (phosphate buffer solution). At pH 1.2 (HCl/KCl buffer solution) and pH 5.6 (distilled water) PRXAH showed statistically higher dissolution rate and total amount dissolved value after 10 h of testing. It can be emphasized that these differences might exist and be more pronounced thus having consequences in overall absorption rates and bioavailability *in vivo*. Unlike with solubility measurements, higher dissolution rate of PRXAH compared to PRXMH was observed at all tested conditions and throughout the testing period. Small differences at the beginning of dissolution experiments might be due to different PRX release rate from hard gelatin capsules. However, an average capsule disintegration times did not vary between the two forms, and the main differences were due to the pH enhancing the drug release from capsules in more acidic environment.

In dissolution studies, the two PRX solid-state forms revealed similar trends and pH dependence as observed in solubility testing. The differences between the two forms were not as obvious as in solubility tests but superior dissolution was observed with PRXAH in all aqueous media and pH conditions. These results could be explained by the differences in the amount of PRX used in solubility and dissolution tests. In case of solubility test, the measurements included an excess of PRX, and consequently, there was a higher driving force for solid-state changes compared to the dissolution rate studies (only 20 mg of PRX in the capsules). In dissolution test, the dissolution rate of PRX was affected by the dissolution media and pH. It is likely that no complete solid-state phase transformation to PRXMH occurred within 45 min of dissolution testing.

3.2.3. *Effect of SLS on the solubility and dissolution of PRX forms*

It is well known that the surface tension in gastric fluid is lower compared to water, which is explained by the presence of surfactants. PRX is an ionizable drug that has low aqueous solubility, and consequently the presence of surfactants (in addition to pH and ionic strength) may change its dissolution characteristics. The effect of SLS as a plasticizer has been recently shown in solid dispersions, where its action is largely dependent on the molecular structure of an API and the polymer (Patel and Joshi, 2008). According to author's knowledge, no study on the effects of SLS on different PRX solid state forms has been published to date. Due to the reasons mentioned above and also due to the known interaction of PRX with SLS (Chakraborty and Sarkar, 2005), the effect of SLS (in different concentrations) was investigated only in distilled water, where the lowest solubility and dissolution rates of PRX forms occurred.

After addition of SLS (1%), the pH of an aqueous solution increased to pH 8. As expected, SLS (together with an increase in pH) enhanced the solubility and dissolution rate of the two PRX forms (Fig. 5a and b). Similar results have been shown for other acidic drugs such as ibuprofen, nimesulide and mefenamic acid (Park and Choi, 2006). This could be explained by the fact that in more alkaline environment weak acids have better solubility and dissolution characteristics. It must be noted that no maximum solubility values could be obtained, since all the material dissolved during the solubility testing in the presence of SLS. The other explanation is the effect of surfactant. The action of surfactant is dual: (1) the solubilization effect and (2) the adsorption of surfactant molecules on the surface of an API, thus enhancing its wettability and solubility. The formation of micelles depends on the pK_a of an API and the ionic nature of surfactant (Park and Choi, 2006). The CMC for SLS has been reported to be 0.2–0.3% (Barreiro-Iglesias et al., 2003). Therefore, when 1% SLS solution in distilled water is used, it is very likely that micelles are formed and thus incorporate undissociated PRX molecules into their structure. In addition, SLS molecules attach to the surface of PRX forms, and consequently could increase the dissolution rate and total amount of dissolved solute. However, PRXMH seemed to be more affected by the presence of SLS since the dissolution rate was increased several folds (Fig. 5b). This kind of result can be explained by the molecular structure differences between the two solid-state forms. In addition, PRXAH has better solubility and dissolution behavior compared to PRXMH which has a huge influence at the beginning of dissolution process. When

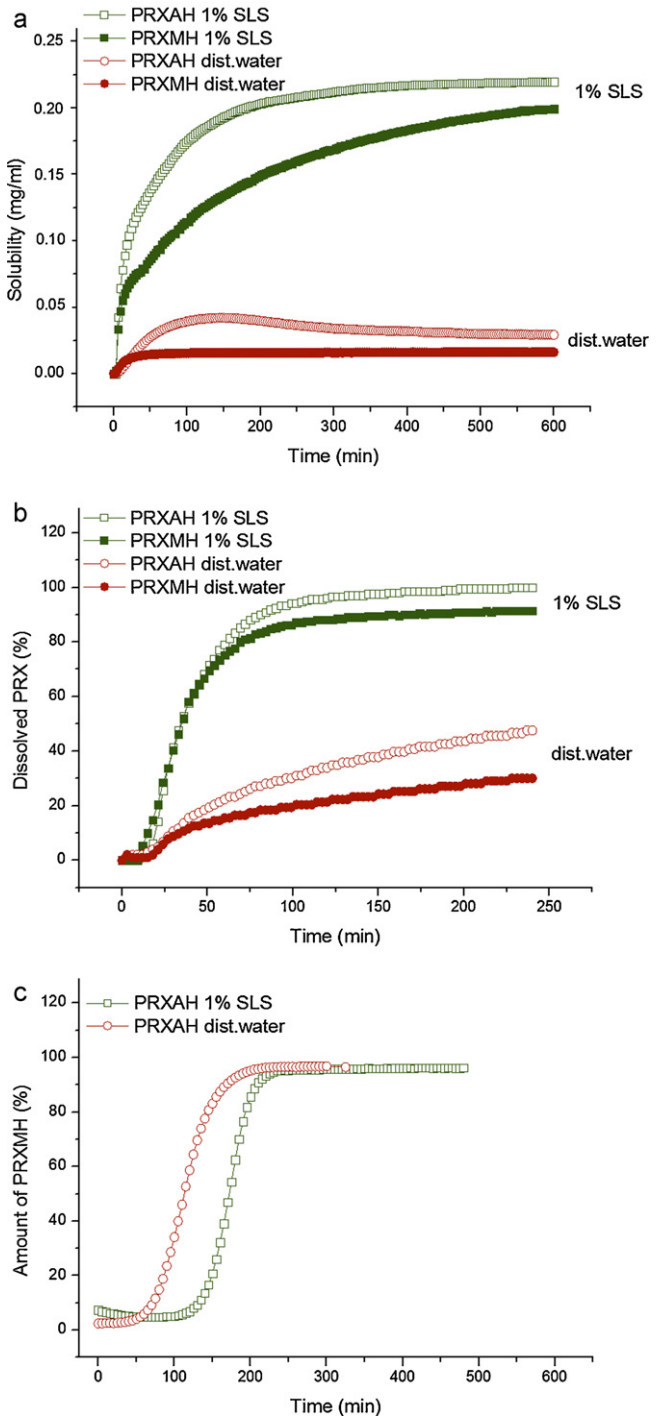

Fig. 5. Effect of surfactant SLS (1%) on the (a) solubility and (b) dissolution of PRXAH (open green squares) and PRXMH (closed green squares) in the presence of 1% SLS in distilled water, comparison with pure distilled water conditions (open and closed red circles for PRXAH and PRXMH, respectively); (c) predicted PRXMH amount (open green squares) in the presence of 1% SLS in distilled water and comparison with pure distilled water conditions (open red circles). (For interpretation of the references to color in this figure legend, the reader is referred to the web version of the article.)

SLS molecules attach to the surface of PRXMH with a zwitterionic structure (or when PRXMH molecules are incorporated into SLS micelles), the solubilization occurs, and consequently the dissolution will be enhanced. In the presence of SLS, PRXAH was totally dissolved in 1% SLS solution whereas in case of pure distilled water (without SLS), only approximately 20% of PRXAH was dissolved. In distilled water, PRX exists in a zwitterionic/neutral form and has the lowest solubility. In addition, parallel phase transformation to PRXMH may also decrease the dissolution rate. The present results showed that SLS enhanced the solubility and dissolution of both PRX solid-state forms, with greater effect on the PRXMH.

As expected, the increase in SLS concentration facilitated the dissolution of an ionizable poorly water-soluble PRX, and this supports also earlier findings reported by Jinno et al. (2000). In addition, the absorption spectra of PRXAH and PRXMH in the presence of SLS revealed that PRX exists in a neutral form, and not an anionic form of API was observed. Presumably, the formed micelles consisted of PRX at a same prototropic form in a solution. Although the surfactant mixtures have been proposed to enhance the solubility and dissolution the most, SLS has been proven to work independently as solubility enhancer due to its micelle formation properties (Patel and Joshi, 2008).

3.3. Solid state changes during slurry testing

3.3.1. Effect of pH on the solid state changes

Since PRX may also exist in different solid-state forms, the dissolution and solubility behavior may be even more complicated. It was of interest to clarify the solid-state transformation phenomena during solubility and dissolution measurements, and therefore *in situ* and in-line Raman spectroscopy monitoring was performed in slurry. These conditions mimicked the ones during solubility testing. Jinno et al. (2000) reported that PRX transforms to yellow PRXMH during solubility testing, but to authors' knowledge this hydrate formation has not been quantitatively investigated at different pHs.

In the present study, PLS model was developed for monitoring the potential solid-state transformations in slurry. Two latent variables were used to build the PLS model, and the first latent variable explained 93.5% of the variations in spectra. The R^2X, R^2Y and Q^2Y values for the PLS model of the Raman spectra were 98.8%, 98.8%, and 98.8%, respectively. The root mean square error of prediction set (RMSEPs) and root mean square error of calibration (RMSEC) were 4.0% and 4.2%, respectively. Even though the model was modified from the previous studies, the scores plot, weight vectors for the first and second latent variable, and the observed *vs* predicted concentrations were similar to those reported before (Kogermann et al., 2008).

A good correlation between the PRX calibration model spectra and real time spectra was obtained. The spectral data obtained from in-line Raman measurements at different pHs were introduced to the PLS model, and the hydrate formation after specified time points in different conditions was predicted by using this model (Fig. 6). Slight differences in the PLS model are derived from differences between the measurement setups and conditions during in-line spectral data collection. Different sources of error associated with quantitative analysis may have an impact when using Raman spectroscopy (Heinz et al., 2007). Spectral data that were used to build the model supported these model predictions. When hydrate formation was first observed, the PRXMH peak at 1401 cm^{-1} started to grow being the most suitable change in spectra that could be monitored (Fig. 1b). After complete hydrate formation no peak shifts or intensity changes in Raman spectra were observed.

It is relatively easy to visually differentiate between anhydrous and hydrate forms due to PRXMH yellow color. The SEM micrographs of hydrate formation in slurry suggest the appearance of PRXMH crystals on the surface of PRXAH after 125 min of testing (shown as Fig. A1). In our experiments, however, Raman spectra and the PLS model revealed that pure PRXMH was not present although the slurry was already yellow (Fig. 6a and b). Spectra and PLS model predictions also revealed that the hydrate formation and its rate (like the solubility and dissolution rate of PRX), were strongly affected by pH (Fig. 6). Fastest hydrate formation occurred at pH

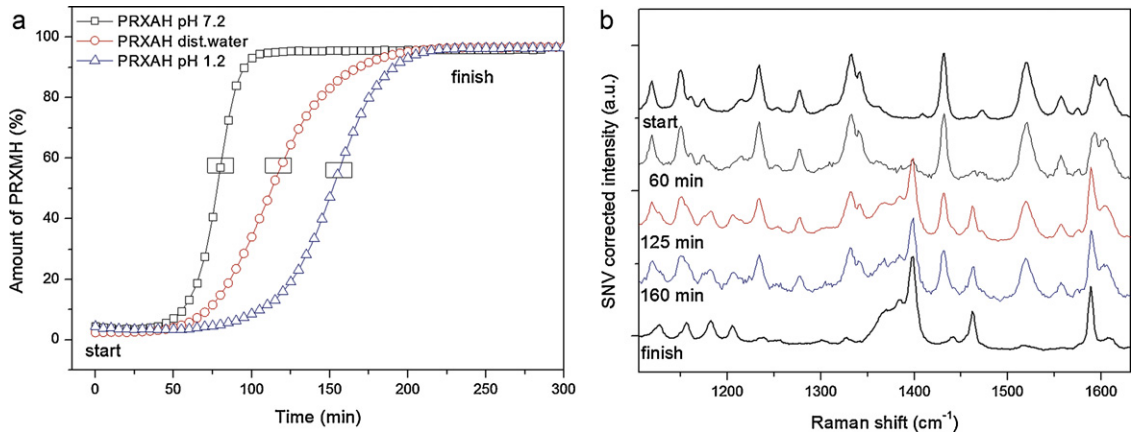

Fig. 6. *In situ* monitoring of phase transformation. (a) PLS model predictions at pH 7.2 (open black squares), distilled water pH 5.6 (open red circles) and pH 1.2 (open blue triangles); (b) Raman spectra of PRXAH at zero point 0 min (start), and after 160 min at pH 1.2, 125 min in distilled water (pH 5.6) and 60 min at pH 7.2, and after complete hydrate (PRXMH) formation (finish). Starting and finish spectra are shown only for distilled water (pH 5.6) since no differences were observed at pH 1.2 or 7.2. The spectra are SNV corrected and offset for clarity.

7.2 (phosphate buffer solution) where changes started approximately after 40 min, and the phase transformation was completed within 115 min of testing. When half of hydrate formation had occurred (60 min of testing), the Raman spectra resembled much more PRXAH than PRXMH, thus indicating very fast phase transformation at the end of testing. The hydrate formation in distilled water (pH 5.6) started after 55 min and transformation had completed after 215 min. The slowest hydrate formation was observed at pH 1.2 (HCl/KCl buffer solution). Changes started after approximately 80 min and complete hydrate formation was obtained after 225 min of testing. Raman spectra obtained at pH 1.2 (HCl/KCl buffer solution) and pH 5.6 (distilled water) revealed lower hydrate formation kinetics compared to the transformation at pH 7.2 (phosphate buffer solution). These results were in good agreement with solubility test findings (also an excess of PRX was used) and complement our understanding on PRXAH behavior at different pHs (Figs. 6 and 7). The solid-state transformation of PRXAH to a PRXMH occurred during solubility study. The fastest hydrate formation occurred at pH 7.2 (phosphate buffer solution), where also the fastest dissolution rate and highest value for total amount of dissolved solute (PRXAH and PRXMH), were observed (Fig. 7). PRX dissolves well in basic environment, and although transformation to PRXMH occurred, the dissolution rate was still the fastest. Solid state transformations at pH 1.2 (HCl/KCl buffer solution) were the slowest, and therefore favoring the dissolution of PRXAH compared to the distilled water conditions. Simultaneously to PRXAH dissolution, also PRXMH formation occurred and slowed down the process. The solid-state phase transformation was found to be faster at pH 5.6 (distilled water) compared to pH 1.2 (HCl/KCl buffer solution) but much slower compared to pH 7.2 (phosphate buffer solution). The dissolution, however, was the slowest for both solid-state forms in distilled water. Interestingly, PRXMH reached the maximum solubility quite fast, and therefore, the fast transformation to PRXMH during solubility measurements also slowed down the dissolution of PRXAH in distilled water. The dissolution and recrystallization from supersaturated solution occur simultaneously which affects the solubility and dissolution characteristics and the solid state transformations of PRXAH.

Hydrate formation is a solvent-mediated transformation that can be divided into three main stages, namely dissolution, nucleation and crystal growth. In the first step, PRXAH will dissolve with specific dissolution rate which largely depends on the pH of the environment, solid state form of API, particle size, surface defects, *etc.* After that the solution will become supersaturated with respect to the PRXMH solubility. Second step is the formation of PRXMH nuclei on the surface of PRXAH (as shown in Fig. A1). Finally, there is a growth step during which PRXMH crystals will grow from nuclei to form larger crystals and this process also proceeds *via* specific kinetics. Previous study has shown that no simple correlation exists between the solid state transformation kinetics and solubility or dissolution rate of APIs (Wikström et al., 2008). It has been shown that the API and its solid form specific properties (*e.g.* solubility, dissolution rate) and also surface properties and external factors (*e.g.* presence of seeds, degree of shear forces) influence the solid state transformation (Lindfors et al., 2007; Wikström et al., 2008). For example the driving force for crystal growth is the level of supersaturation along with the solute diffusion coefficient, temperature and the molecular surface energy of the crystal surface interface (Rodriguez-Hornedo and Wu, 1991; Wikström et al., 2008). The crystal growth is slower than dissolution even when equal driving forces are applied (Lindfors et al., 2007).

3.3.2. *Effect of SLS on the solid-state changes*

The solid-state changes of PRXAH were also monitored in the presence of SLS to get an insight into the impaired dissolution characteristics of API in distilled water and the possible solubilizing effect of SLS. Raman spectroscopic monitoring revealed that PRXAH conversion to PRXMH had slowed down in the presence of SLS (Fig. 8). SLS inhibited the start of PRXMH nucleation on the surface of PRXAH and therefore the transformation of PRXAH to PRXMH was observed 40 min later in the SLS containing solution compared to that observed in pure distilled water with pH 5.6 (Fig. 5c). In addition, no morphology change of PRXMH was observed in the presence of SLS, although the crystals were smaller compared to pure recrystallized PRXMH (shown as Fig. A2). It must be noted, that in the presence of SLS at different pHs also different transformation kinetics were observed and transformation was totally inhibited at pH 1.2 (HCl/KCl buffer solution) (shown as Fig. A3). No straight comparison can be made with solubility experiments and slurry tests, since in slurry tests much higher PRX concentration (400 mg/ml *vs* 0.22 mg/ml) was used compared to solubility testing conditions. It is evident that the amount of PRX plays the key role in this process. Since all the material dissolved during solubility and dissolution studies, it is evident that there was not enough time or any driving force for the solid-state changes at these lower PRXAH concentrations. However, some insight into the possible mechanism of action can be made and conclusions drawn using slurry studies.

Interestingly, the present results verified that solubility and dissolution is more favored in the presence of SLS (*i.e.* solid-state changes occurred more slowly). Most likely SLS (above

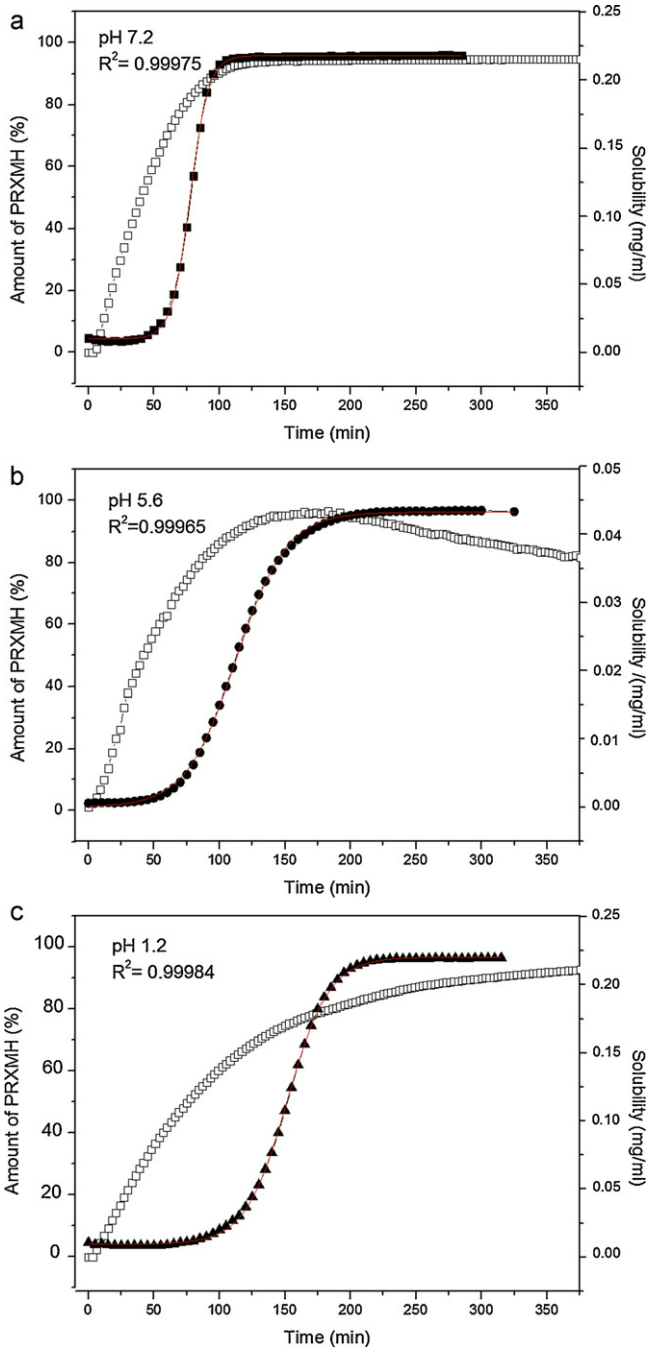

Fig. 7. (a) Predicted PRXMH amount (closed squares) and solubility-time profile of PRXAH (open squares) at pH 7.2, (b) predicted PRXMH amount (closed circles) and solubility-time profile of PRXAH (open circles) in distilled water (pH 5.6), and (c) predicted PRXMH amount (closed triangles) and solubility-time profile of PRXAH (open triangles) at pH 1.2. Model fitting by Boltzmann equation: $y = A_2 + (A_1 - A_2)/(1 + \exp((x - x_0)/dx)$ with respective R^2.

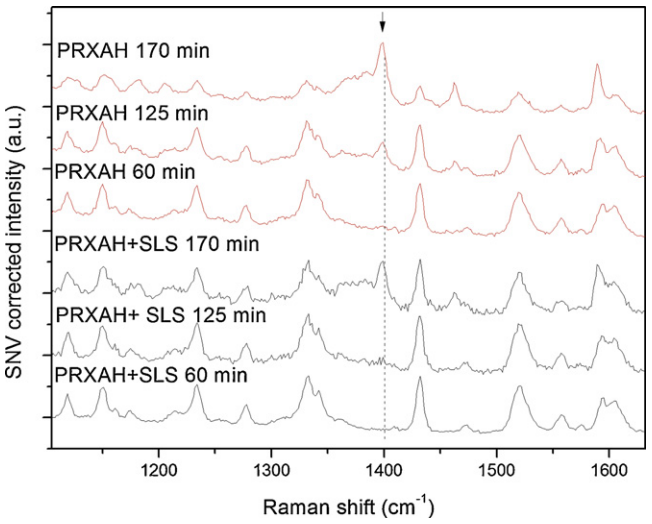

Fig. 8. SNV corrected Raman spectra of PRXAH in distilled water pH 5.6 (red) and 1% SLS solution (black) at different time-points during slurry testing. Characteristic PRXMH peak at 1401 cm^{-1} is shown with an arrow. (For interpretation of the references to color in this figure legend, the reader is referred to the web version of the article.)

CMC) affects supersaturation *via* solubilizing effect, and thus PRX solubility increases and the solution is kept supersaturated longer without seeing any nucleation. It is known that the nucleation rate itself depends largely on the temperature, degree of supersaturation and interfacial tension. Furthermore, the presence of surfactant is known to reduce the surface tension and increase the rate of less soluble form nucleation. However, similar kind of nucleation inhibition has been reported previously for Tween 80 (Chen et al., 2003). Chen et al. (2003) showed that when surfactant is used above its CMC, the effect of reduced surface tension on nucleation is negated by an increase in viscosity or adsorption of surfactant on the crystal surface. Totally opposite behavior has been reported with carbamazepine (CBZ) in SLS solutions (Luhtala, 1992; Rodriguez-Hornedo and Murphy, 2004). Rodriguez-Hornedo and Murphy (2004) reported that SLS decreased the threshold concentration for nucleation, increased the CBZ dihydrate crystallization rate on the surface of CBZ anhydrate below the CMC and increased CBZ dihydrate nucleation rate in a solution above the CMC. Lehto et al. (2009) showed that another important surfactant, sodium taurocholate (STC), may inhibit the CBZ dihydrate formation due to strong hydrogen bonding between CBZ and STC molecules. According to Rodriguez-Hornedo and Murphy (2004), STC promotes CBZ dihydrate crystallization in a solution together with CBZ dihydrate morphology change. They suggested that the action of surfactant in the solid state transformation is very much dependent on the solid-state form and amount of API, amount of surfactant in a solution, and testing conditions.

4. Conclusions

The two solid-state forms of PRX, PRXMH and PRXAH, show different solubilities and dissolution rates at pH 1.2 (HCl/KCl buffer solution), pH 5.6 (distilled water) and pH 7.2 (phosphate buffer solution). This is derived from their different molecular structures and ionization of the molecules. For the first time PRXMH formation was quantified in slurry using Raman spectroscopy together with PLS regression. This method allowed explaining the solubility-time profiles of PRXAH in different environments during solubility testing. The enhanced solubility and dissolution rate of PRXAH and PRXMH in the presence of SLS could be explained by the dual action of SLS (solubilization and adsorption on the surface) as well as delayed solid-state changes of API during solubility testing. Thus SLS action depends also very much on the solid-state form of an API and its molecular structure. This study gains an understanding on the hydrate formation of PRX in biologically relevant conditions. The results obtained reveal that the different solubility and dissolution behavior of PRX solid-state forms, pH of dissolution medium and presence of SLS affect the kinetics of solid-state transformation. It is important that these parameters are carefully considered when polymorphic APIs are being tested in conventional *in vitro* dissolution tests.

Acknowledgements

The work is part of the targeted financing project no SF0180042s09 and ETF grant project no ETF7980. Estonian Ministry of Education and Research is acknowledged for financial support. This research was supported by European Social Fund's Doctoral Studies and Internationalization Programme DoRa since September 1, 2010. Dr. J. Aruväli and Prof K. Kirsimäe (X-ray laboratory, Institute of Ecology and Earth Sciences, University of Tartu), and Prof. V. Sammelselg and PhD student J. Kozlova (Institute of Physics, University of Tartu) are acknowledged for the XRPD and SEM experiments, respectively. Dr A. Meos (Department of Pharmacy, University of Tartu) is thanked for conducting the UV-Vis spectroscopy measurements. Prof C. H. Schwalbe (Aston Pharmacy School, Aston University, UK) is acknowledged for useful discussions regarding this work. MSc Pharmacy students Pille Mägar and Nadezhda Ruina are thanked for performing the dissolution and slurry tests, respectively.

Appendix A. Supplementary data

Supplementary data associated with this article can be found, in the online version, at http://dx.doi.org/10.1016/j.ijpharm.2012.04.042.

References

Aaltonen, J., Heinänen, P., Peltonen, L., Kortejärvi, H., Tanninen, V.P., Christiansen, L., Hirvonen, J., Yliruusi, J., Rantanen, J., 2006. In situ measurement of solvent-mediated phase transformations during dissolution testing. J. Pharm. Sci. 95, 2730–2737.

Airaksinen, S., Karjalainen, M., Kivikero, N., Westermarck, S., Shevchenko, A., Rantanen, J., Yliruusi, J., 2005. Excipient selection can significantly affect solid-state phase transformation in formulation during wet granulation. AAPS PharmSci. Tech. 6, E311–E322.

Amidon, G.L., Lennernas, H., Shah, V.P., Crison, J.R., 1995. A theoretical basis for a biopharmaceutic drug classification: the correlation of in vitro drug product dissolution and in vivo bioavailability. Pharm. Res. 12, 413–420.

Banerjee, R., Sarkar, M., 2002. Spectroscopic studies of microenvironment dictated structural forms of piroxicam and meloxicam. J. Lumin. 99, 255–263.

Banerjee, R., Chakraborty, H., Sarkar, M., 2003. Photophysical studies of oxicam group of NSAIDs: piroxicam, meloxicam and tenoxicam. Spectrochim. Acta, Part A 59, 1213–1222.

Barreiro-Iglesias, R., Alvarez-Lorenzo, C., Concheiro, A., 2003. Poly(acrylic acid) microgels (carbopol® 934)/surfactant interactions in aqueous media. Part II: ionic surfactants. Int. J. Pharm. 258, 179–191.

Bhattachar, S.N., Risley, D.S., Werawatganone, P., Aburub, A., 2011. Weak bases and formation of a less soluble lauryl sulfate salt/complex in sodium lauryl sulfate (SLS) containing media. Int. J. Pharm. 412, 95–98.

Bordner, J., Richards, J.A., Weeks, P., Whipple, E.B., 1984. Piroxicam monohydrate: a zwitterionic form, $C_{15}H_{13}N_3O_4S^*H_2O$. Acta Crystallogr. C40, 989–990.

Brouwers, J., Brewster, M.E., Augustijns, P., 2009. Supersaturating drug delivery systems: the answer to solubility-limited oral bioavailability? J. Pharm. Sci. 98, 2549–2572.

Chakraborty, H., Sarkar, M., 2005. Interaction of piroxicam with micelles: effect of hydrophobic chain length on structural switchover. Biophys. Chem. 117, 79–85.

Chakraborty, S., Shukla, D., Jain, A., Mishra, B., Singh, S., 2009. Assessment of solubilization characteristics of different surfactants for carvedilol phosphate as a function of pH. J. Colloid Interface Sci. 335, 242–249.

Chen, L.R., Wesley, J.A., Bhattachar, S., Ruiz, B., Bahash, K., Babu, S.R., 2003. Dissolution behavior of a poorly water soluble compound in the presence of Tween 80. Pharm. Res. 20, 797–801.

De Smidt, J.H., Fokkens, J.G., Grijseels, H., Crommelin, D.J.A., 1986. Dissolution of theophylline monohydrate and anhydrous theophylline in buffer solutions. J. Pharm. Sci. 75, 497–501.

Gwak, H.S., Choi, J.S., Choi, H.K., 2005. Enhanced bioavailability of piroxicam via salt formation with ethanolamines. Int. J. Pharm. 297, 156–161.

Heinz, A., Savolainen, M., Rades, T., Strachan, C.J., 2007. Quantifying ternary mixtures of different solid state forms of indomethacin by Raman and near-infrared spectroscopy. Eur. J. Pharm. Sci. 32, 182–192.

Jinno, J., Oh, D.M., Crison, J.R., Amidon, G.L., 2000. Dissolution of ionizable water-insoluble drugs: the combined effect of pH and surfactant. J. Pharm. Sci. 89, 268–274.

Jørgensen, A., Rantanen, J., Karjalainen, M., Khriachtchev, L., Räsänen, E., Yliruusi, J., 2002. Hydrate formation during wet granulation studied by spectroscopic methods and multivariate analysis. Pharm. Res. 19, 1285–1291.

Kogermann, K., Aaltonen, J., Strachan, C.J., Pöllänen, K., Veski, P., Heinämäki, J., Yliruusi, J., Rantanen, J., 2007. Qualitative in situ analysis of multiple solid-state forms using spectroscopy and partial least squares discriminant modeling. J. Pharm. Sci. 96, 1802–1820.

Kogermann, K., Aaltonen, J., Strachan, C.J., Pöllänen, K., Heinämäki, J., Yliruusi, J., Rantanen, J., 2008. Establishing quantitative in-line analysis of multiple solid-state transformations during dehydration. J. Pharm. Sci. 97, 4983–4999.

Kojic-Prodic, B., Ruzic-Toros, Z., 1982. Structure of piroxicam. Acta Crystallogr. B38, 2948.

Koradia, V., De Lemos, A.F.F., Allensø, M., De Diego, H.L., Ringkjøbing-Elema, M., Müllertz, A., Rantanen, J., 2011. Phase transformations of amlodipine besylate solid forms. J. Pharm. Sci. 100, 2896–2910.

Kozjek, F., Golic, L., Zupet, P., Palka, E., Vodopivec, P., Japelj, M., 1985. Physicochemical properties and bioavailability after oral absorption of two crystal forms of piroxicam. Acta Pharm. Jugosl. 35, 275–281.

Lehto, P., Aaltonen, J., Tenho, M., Rantanen, J., Hirvonen, J., Tanninen, V.P., Peltonen, L., 2009. Solvent-mediated solid phase transformations of carbamazepine: effects of simulated intestinal fluid and fasted state simulated intestinal fluid. J. Pharm. Sci. 98, 985–996.

Lindfors, L., Skantze, P., Skantze, U., Westergren, J., Olsson, U., 2007. Amorphous drug nanosuspensions. 3. Particle dissolution and crystal growth. Langmuir 23, 9866–9874.

Luhtala, S., 1992. Effect of sodium lauryl sulphate and polysorbate 80 on crystal growth and aqueous solubility of carbamazepine. Acta Pharm. Nord. 4, 85–90.

Nogami, H., Nagai, T., Yotsuyanagi, T., 1969. Dissolution phenomena of organic medicinals involving simultaneous phase changes. Chem. Pharm. Bull. 17.

Okuyama, H., Ikeda, Y., Kasai, S., Imamori, K., Takayama, K., Nagai, T., 1999. Influence of non-ionic surfactants, pH and propylene glycol on percutaneous absorption of piroxicam from cataplasm. Int. J. Pharm. 186, 141–148.

Otsuka, M., Teraoka, R., Matsuda, Y., 1992. Rotating-disk dissolution kinetics of nitrofurantoin anhydrate and monohydrate ar various temperatures. Pharm. Res. 9, 307–311.

Otsuka, M., Hasegawa, H., Matsuda, Y., 1997. Effect of polymorphic transformation during the extrusion-granulation process on the pharmaceutical properties of carbamazepine granules. Chem. Pharm. Bull. 45, 894–898.

Park, S.H., Choi, H.K., 2006. The effects of surfactants on the dissolution profiles of poorly water-soluble acidic drugs. Int. J. Pharm. 321, 35–41.

Patel, A.R., Joshi, V.Y., 2008. Evaluation of SLS:APG mixed surfactant systems as carrier for solid dispersion. AAPS PharmSci. Tech. 9, 583–590.

Reck, G., Laban, G., 1990. Prediction and establishment of a new crystalline piroxicam modification. Pharmazie 45, 257–259.

Reck, G., Dietz, G., Laban, G., Günther, W., Bannier, G., Höhne, E., 1988. X-ray studies on piroxicam modifications. Pharmazie 43, 477–481.

Rodriguez-Hornedo, N., Murphy, D., 2004. Surfactant-facilitated crystallization of dihydrate carbamzepine during dissolution of anhydrous polymorph. J. Pharm. Sci. 93, 449–460.

Rodriguez-Hornedo, N., Wu, H.J., 1991. Crystal growth kinetics of theophylline monohydrate. Pharm. Res. 8, 643–648.

Sheth, A.R., Bates, S., Muller, F.X., Grant, D.J.W., 2004. Polymorphism in piroxicam. Cryst. Growth Des. 4, 1091–1098.

Sheth, A.R., Lubach, J.W., Munson, E.J., Muller, F.X., Grant, D.J.W., 2005. Mechanochromism of piroxicam accompanied by intermolecular proton transfer probed by spectroscopic methods and solid-state changes. J. Am. Chem. Soc. 127, 6641–6651.

Shihab, F.A., Ebian, A.R., Mustafa, R.M., 1979. Effect of polyethylene glycol, sodium-laurylsulfate and polysorbate-80 on the solubility of furosemide. Int. J. Pharm. 4, 13–20.

Vrečer, F., Vrbinc, M., Meden, A., 2003. Characterization of piroxicam crystal modifications. Int. J. Pharm. 256, 3–15.

Wikström, H., Marsac, P.J., Taylor, L.S., 2005. In-line monitoring of hydrate formation during wet granulation using Raman spectroscopy. J. Pharm. Sci. 94, 209–219.

Wikström, H., Rantanen, J., Gift, A.D., Taylor, L.S., 2008. Toward an understanding of the factors influencing anhydrate-to-hydrate transformation kinetics in aqueous environments. Cryst. Growth Des. 8, 2684–2693.

Yazdanian, M., Briggs, K., Jankovsky, C., Hawi, A., 2004. The "high solubility" definition of the current FDA guidance on biopharmaceutical classification system may be too strict for acidic drugs. Pharm. Res. 21, 293–299.

Zhang, J., Li, G.Z., 2004. Phase behavior of APG/alcohol/alkane/water mixture. J. Disper. Sci. Tech. 25, 27–34.

Zhang, G.Z.Z., Law, D., Schmitt, E.A., Qiu, Y., 2004. Phase transformation considerations during process development and manufacture of solid oral dosage forms. Adv. Drug Deliv. Rev. 56, 371–390.

Zimmermann, A., Tian, F., Lopez de Diego, H., Elema, M.R., Rantanen, J., Müllertz, A., Hovgaard, L., 2008. Influence of the solid form of siramesine hydrochloride on its behavior in aqueous environments. Pharm. Res. 26, 846–854.